ELSEVIER

Journal of Neuroscience Methods 129 (2003) 95–104

JOURNAL OF NEUROSCIENCE METHODS

www.elsevier.com/locate/jneumeth

A dynamic recurrent neural network for multiple muscles electromyographic mapping to elevation angles of the lower limb in human locomotion

G. Cheron [a,b,*], F. Leurs [a], A. Bengoetxea [a], J.P. Draye [b,c], M. Destrée [a], B. Dan [d]

[a] *Laboratory of Movement Biomechanics, ISEPK, Université Libre de Bruxelles, Avenue P. Héger, CP 168, Brussels 1050, Belgium*
[b] *Laboratory of Electrophysiology, Université de Mons-Hainaut, Waterloo Office Park, Building K, Drève Richelle 161, 1410 Waterloo, Belgium*
[c] *Avaya Belgium salnv, Waterloo Office Park, Building K, Drève Richelle 161, 1410 Waterloo, Belgium*
[d] *Department of Neurology, University Children's Hospital Queen Fabiola, Brussels, Belgium*

Received 25 February 2003; received in revised form 26 May 2003; accepted 27 May 2003

Abstract

This paper describes the use of a dynamic recurrent neural network (DRNN) for simulating lower limb coordination in human locomotion. The method is based on mapping between the electromyographic signals (EMG) from six muscles and the elevation angles of the three main lower limb segments (thigh, shank and foot). The DRNN is a fully connected network of 35 hidden units taking into account the temporal relationships history between EMG and lower limb kinematics. Each EMG signal is sent to all 35 units, which converge to three outputs. Each output neurone provides the kinematics of one lower limb segment. The training is supervised, involving learning rule adaptations of synaptic weights and time constant of each unit. Kinematics of the locomotor movements were recorded and analysed using the opto-electronic ELITE system. Comparative analysis of the learning performance with different types of output (position, velocity and acceleration) showed that for common gait mapping velocity data should be used as output, as it is the best compromise between asymptotic error curve, rapid convergence and avoidance of bifurcation. Reproducibility of the identification process and biological plausibility were high, indicating that the DRNN may be used for understanding functional relationships between multiple EMG and locomotion. The DRNN might also be of benefit for prosthetic control.

Keywords: Locomotion; Artificial neural network; Electromyography; Kinematics; Movement simulation

1. Introduction

In human locomotion electromyographic activity (EMG) is the only non-invasively accessible signal directly related to the final command of movement. EMG signal, though not ideal, is a reasonable reflection of the firing rate of a motoneuronal pool (Soechting and Flanders, 1997). The analysis of rectified EMG envelopes of multiple muscles may reveal the basic motor coordination dynamics (Scholz and Kelso, 1990). The relationship between lower limb muscle EMG and support as well as forward progression has been studied (Neptune et al., 2001).

Despite the recent development of artificial neural networks using multiple EMG time course as input for providing joint torque (Koike and Kawato, 1995; Savelberg and Herzog, 1997), joint angular acceleration (Koike and Kawato, 1994; Draye et al., 2002) or position (Cheron et al., 1996) of the upper limb, this type of mapping has sparsely been used in the field of human locomotion (Sepulveda et al., 1993).

Conceptual and technical problems could explain why the neural network approach has been limited in the field of locomotion studies. Walking movement, although seemingly stereotyped, is highly complex as it integrates equilibrium constraints and forward propulsion in a multi-joint system. Therefore separate feedforward neural models could be developed, one for

* Corresponding author. Tel.: +32-2-650-2187; fax: +32-2-650-3745.
E-mail address: gcheron@ulb.ac.be (G. Cheron).

0165-0270/03/$ - see front matter
doi:10.1016/S0165-0270(03)00167-5

postural control and one for propulsion movement implicating some gating or selecting devices for an appropriate switch between these different networks. However, although this type of approach has proved successful for arm movement control (Koike and Kawato, 1994), it is problematic for the control of task with simultaneous postural and movement requirements such as locomotion where distinction between the two modes of control is difficult on the basis of EMG signals. Moreover, in walking the great number of joints and body segments involved pose the problem of choice of the kinematic parameter to be used as the output of the neural mapping.

Technically, the majority of neural networks used for EMG-to-kinematics mapping have been of the feedforward type (Sepulveda et al., 1993; Koike and Kawato, 1994). In these networks information flows from the input neurones to the output neurones without any feedback connections. This excludes context and historical information, which are thought to be crucial in motor control (Kelso, 1995). In contrast, recurrent neural networks take these aspects into account and are recognised as universal approximators of dynamical systems (Hornik et al., 1989; Doya, 1993). Therefore, they seem particularly relevant to the study of motor control (Draye et al., 2001, 2002).

In this study we propose a new tool for the study of the lower limb EMG signals associated with locomotion using a dynamic recurrent neural network (DRNN). This neural network is original because it takes into account the history of the temporal relationships between raw EMG signals from six muscles and the elevation angles of the three main segments of the lower limb. Elevation angles of the thigh, shank and foot were chosen because they represent robust parameters of human locomotion (Borghese et al., 1996; Lacquaniti et al., 1999) including in children (Cheron et al., 2001a).

2. Materials and methods

2.1. Subjects

The DRNN methodology was applied on EMG and kinematics data recorded in nine healthy adults (five females and four males, 35 ± 6 (mean $\pm$S.D.) years old). Informed consent was obtained from all subjects. The procedures were approved by the local ethics committee of the University and conformed with the Declaration of Helsinki.

2.2. Locomotor task

The subjects were asked to walk barefoot as naturally as possibly, looking straightforward from one end of the ground band to the other end.

2.3. Data recordings

2.3.1. Kinematics

Kinematics of the locomotor movements was recorded and analysed using the opto-electronic ELITE system (Ferrigno and Pedotti, 1985). This system consists of five CCD-cameras detecting retro-reflective markers using a sampling rate of 100 Hz. The cameras were placed 4 m around the progression line of the subjects, 3 m above the floor. After calibration, two-dimensional data were corrected for optical distortion and converted to 3D coordinates according to Borghese et al. (1996).

The position in space of ten passive markers, including nine links, was recorded. Spherical reflective markers (1.5 cm in diameter) were fastened on to the skin overlying the following bony landmarks: the nose at the horizontal extent of the lower border of the orbit, the meatus of the ear, the acromial process, the lateral condyle of the elbow, the styloid process of the wrist, the tubercle of the antero-superior iliac crest, the greater trochanter, the lateral condyle of the knee, the lateral malleolus and the 5th metatarsal.

After reconstruction of the stick diagrams representing successful locomotion of subjects, we focused our analysis on the lower limb segments with respect to the vertical. The movement of the following segments was analysed: trunk (defined by the line connecting the acromion and the iliac spine markers), thigh (trochanter–knee), shank (knee–lateral malleolus) and foot (lateral malleolous–5th metatarsal head). The elevation angles of the thigh, shank and foot in the sagittal plane are noted α_t, α_s and α_f, respectively.

2.3.2. EMG recordings

Surface electromyographic activity (EMG) was recorded with the TELEMG system (BTS, Milan), which is compatible with the ELITE system, so that EMG recordings could be synchronised with kinematic ones in order to study temporal relationships. Raw EMG signals (differential detection) were pre-amplified (1000 times) and transmitted to the main unit with a telemetry system (portable unit). After this, EMG were bandpass filtered (5–2000 Hz), digitised at 1 KHz and then-full wave rectified and smoothed by means of a third order averaging filtre with a time constant of 20 ms. We used standard clip-type adhesive pre-gelled disposable silver–silver chloride electrodes. The electrodes were positioned at an inter-electrode distance of 2.5 cm over the belly of the following six muscles of the left lower limb: rectus femoris (RF), vastus lateralis (VL), biceps femoris (BF), tibialis anterior (TA), gastrocnemius lateral (GL), soleus (SOL).

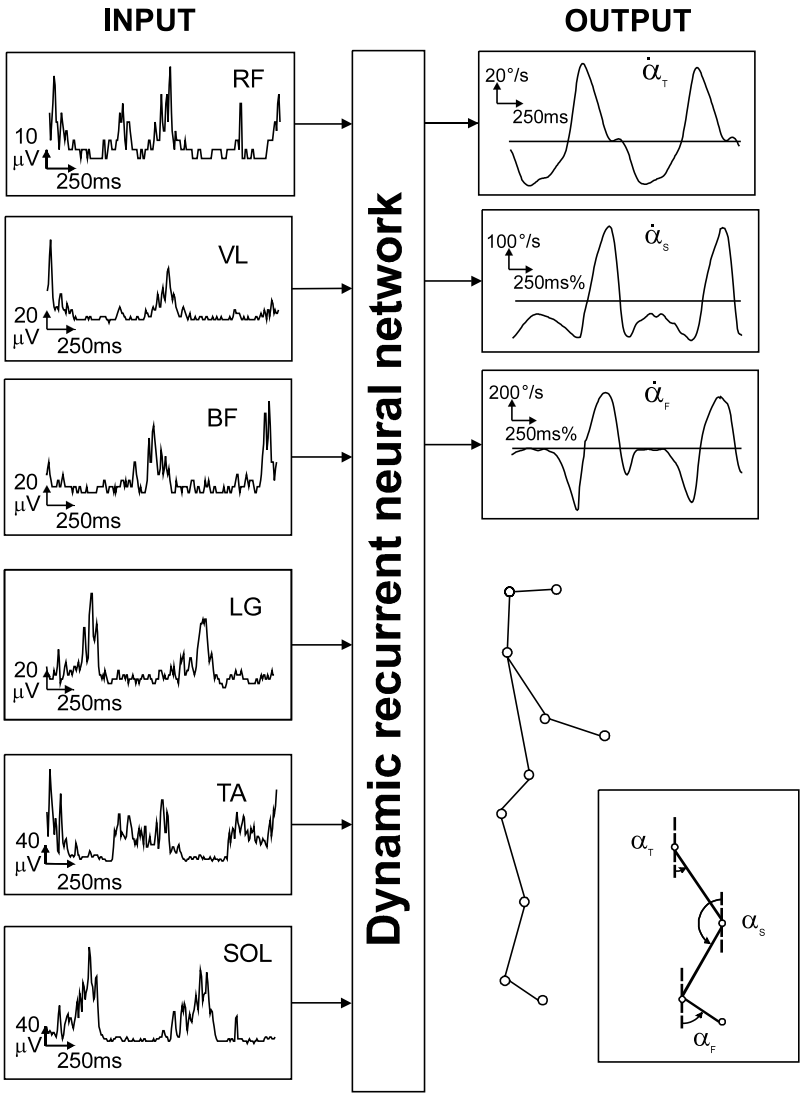

Fig. 1. Input–output relationships of the DRNN. The central box symbolises the DRNN. Each EMG signal is sent to all 35 artificial neurones (hidden unit) which converge to three output units acting merely as summation units. Each output neurone provides one specific type of kinematic data represented by the absolute angles of elevation of the thigh (α_T), shank (α_S) and foot (α_F) with respect to the vertical as indicated in the stick diagram of the insert. The open circles represent the placement of the passive markers.

2.4. Network structure and learning equation

The present DRNN is adapted from a previous version originally developed for the upper limb (Cheron et al., 1996; Draye et al., 1996).

We consider a neural network model governed by the following equations:

$$T_i \frac{dy_i}{dt} = -y_i + F(x_i) + I_i \quad (1)$$

where $F(\alpha)$ is the squashing function $F(\alpha) = (1 + e^{-\alpha})^{-1}$, y_i is the state or activation level of unit i, I_i is an external input (or bias), and x_i is given by:

$$x_i = \sum_j w_{ij} y_j \quad (2)$$

which is the propagation equation of the network (x_i is called the total or effective input of the neuron, W_{ij} is the synaptic weight between units i and j). The time constants T_i will act like a relaxation process. The correction of the time constants will be included in the learning process in order to increase the dynamical features of the model. Introduction of T_i allows more complex frequential behaviour, improves the non-linearity effect of the sigmoid function and the memory effect of time delays (Draye et al., 1995).

The network consists of 35 fully-connected neurones. Therefore, each neurone in an n neurone network has n connections (including a self-connection).

In order to make the temporal behaviour of the network explicit, an error function is defined as:

$$E = \int_{t_0}^{t_1} q(y(t),\ t)\ \mathrm{d}t \tag{3}$$

where t_0 and t_1 give the time interval during which the correction process occurs. The function $q(\mathbf{y}(t), t)$ is the cost function at time t which depends on the vector of the neurone activations $\mathbf{y}$ and on time. We then introduce new variables p_i (called adjoint variables) that will be determined by the following system of differential equations:

$$\frac{\mathrm{d}p_i}{\mathrm{d}t} = \frac{1}{T_i}\ p_i - e_i - \sum_j \frac{1}{T_i}\ w_{ij} F'(x_j) p_j \tag{4}$$

with boundary conditions $p_i(t_1) = 0$. After the introduction of these new variables, we can derive the learning equations:

$$\frac{\delta E}{\delta w_{ij}} = \frac{1}{T_i} \int_{t_0}^{t_1} y_i F'(x_j) p_j\ \mathrm{d}t \tag{5}$$

$$\frac{\delta E}{\delta T_i} = \frac{1}{T_i} \int_{t_0}^{t_1} p_i \frac{\mathrm{d}y_i}{\mathrm{d}t} \tag{6}$$

These equations were originally established by Pearlmutter (1989). Due to the integration of the system of (4) backward through time, this algorithm is sometimes called 'backpropagation through time'.

In order to reduce the time of the learning process, the acceleration method of Silva and Almeida (1990) was used, where each weight and time constant has its own adaptative learning rate.

The training of the network is supervised: the input signals consist of the EMG signals of eight muscles, the output signals consist of the angular velocities of elevation angles of thigh, shank and foot. Each training was associated to only one subject and one type of electrodes location. The error is given by the differential area between the experimental and simulated velocities.

3. Results

Fig. 1 illustrates the input–output relationships of the DRNN. The central box symbolises the DRNN. Each EMG signal is sent to all the 35 artificial neurones (hidden unit) which converge to three output units acting merely as summation units. Each output neurone provides one specific type of kinematic data (in the illustrated situation: the angular velocity of the thigh, shank and foot).

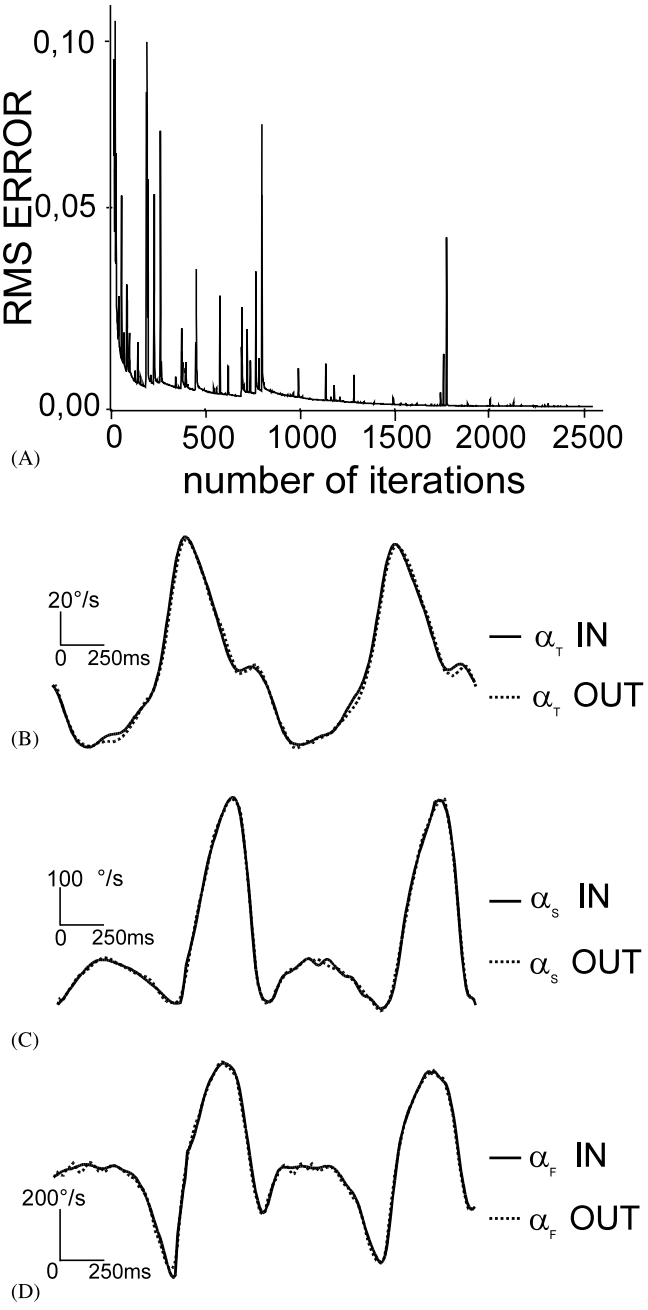

Fig. 2. Assessment of successful learning. (A) Error curve of one learning trial reaching an error value of 0.001 after 5000 iterations. (B, C and D) Superimposition of experimental (—) and DRNN (· · ·) output signals when training reaches an error value of 0.001.

3.1. Criteria for successful learning

Successful learning was ascertained on the basis of the comparison between the DRNN output and the actual output (provided by experimental data). Fig. 2 illustrates the superimposition of these data (Fig. 2B–D) when the training has reached an error value of 0.001. The learning performance was examined on-line by inspection of the error curve (Fig. 2A). The learning process was carried out for 5000 iterations.

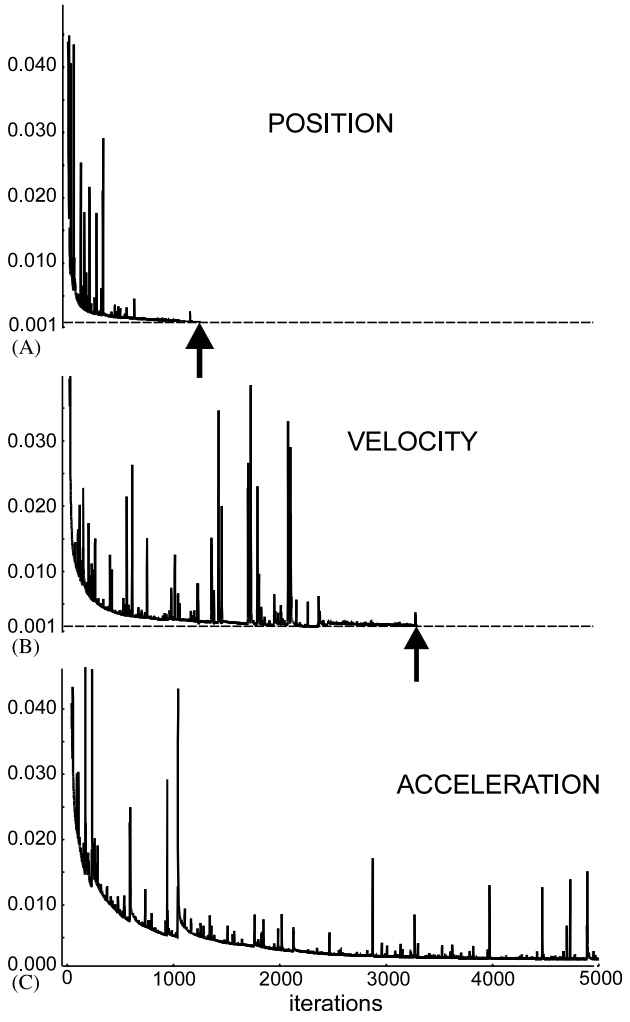

Fig. 3. Choice of the output data. Comparison of error curves corresponding to learning of position (A), velocity (B) and acceleration (C) signals. Note that the error curve related to the position reached 0.001 (arrow) earlier than that related to velocity. The error curve related to acceleration never reached 0.001 during 5000 iterations.

Table 1
Proportion of each type of error curve encountered ($n = 60$)

Error curve	Acceleration	Velocity	Position
No learning	58.4%	21.6%	0.00%
Bifurcation	0.00%	26.6%	83.3%
Asymptotic	41.6%	51.6%	16.6%
Reaching 0.001	0.00%	11.6%	16.6%

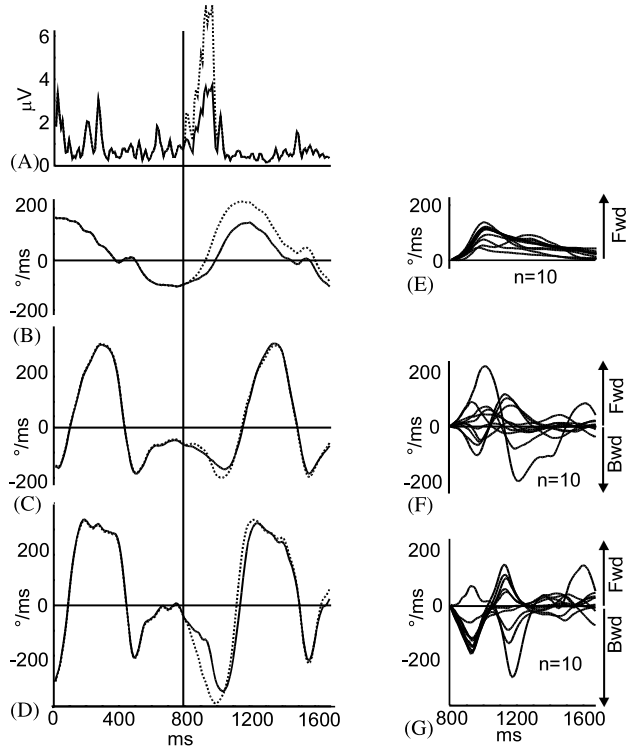

Fig. 4. (A–G) Reproducibility of the identification process. Comparison between ten different successful learning trials. (A) The rectified EMG signal of the soleus muscle, is selectively amplified ($\times 2$) during the major stance phase (STP), (between 35 and 52% of the gait cycle). Superimposition of the velocity profile of the thigh (B), shank (C) and foot (D) after artificial potentiation of the soleus muscle. In order to quantify the effect of the artificial modification of the EMG on the velocity profile we systematically subtracted the initial curve to the modified one. Superimposition of curves resulting from subtraction of the initial curve from the modified one in ten different learning trials for the thigh (E), shank (F) and foot (G).

Unsuccessful learning was characterised by absence of a typical asymptotic error curve. Either the error values remain constant throughout the 5000 iterations, in which case it was considered that there was no learning, or the error curve rapidly diminished during the first 500 iterations and then stabilised at a constant value for the remaining iterations, indicating a bifurcation. Analysis of the corresponding output showed that the DRNN only converged to one or two kinematic curves leaving the other curves untreated.

3.2. Choice of the ouput data

The choice of the ideal output largely depends on the final aim of DRNN use. If the purpose of using the DRNN is to reproduce relevant relationships in human locomotion, kinematic invariant such as elevation angle can be used. However, in this case at least three possibilities can be considered, namely position, velocity and acceleration data.

In order to determine the output data that gives rise to the best learning process, we repeated 60 learning phases respectively for the position, velocity and acceleration data acquired during the same trial executed by a subject and representing two complete walking cycles. For each learning process, we limited the maximum number of iterations to 5000, which takes about 30 min on a PENTIUM II.

Table 2
Reproducibility scores (RS) of the identification process during major stance phase (STP) and major swing phase (SWP) for the six analysed muscles: rectus femoris (RF), vastus lateralis (VL), biceps femoris (BF), gastrocnemius lateralis (GL), tibialis anterior (TA) and soleus (SOL)

Muscles	RS(%) foot		RS(%) shank		RS(%) thigh	
	STP	SWP	STP	SWP	STP	SWP
RF	100	90	90	90	80	90
VL	90	80	90	100	90	100
BF	100	100	60	80	100	100
GL	50	80	90	60	90	100
TA	90	90	90	100	70	100
SOL	90	100	50	100	100	100

Fig. 3 shows a representative asymptotic error curve for each learning paradigm (position, velocity, acceleration). The error curve related to position identification reached the 0.001 limit (1409 ± 229 iterations) ($n = 10$) much earlier than the velocity error curve (4098 ± 566 iterations) ($n = 7$). The error curve related to acceleration identification never reached 0.001 over 5000 iterations.

Table 1 shows the proportion of each type of error curve encountered.

This analysis shows that for common gait mapping velocity data should be used as output, as it is the best compromise between asymptotic error curve shape, rapid convergence and avoidance of bifurcation.

3.3. Reproducibility of the identification process

Reproducibility of the identification process was studied using the mapping data (EMG to angular velocity of the thigh, shank and foot elevation) of one representative subject. The identification process of ten different successful learning trials (asymptotic error of 0.001 reached after a mean ($\pm$S.D.) of 3.330 ($\pm$873) iterations) were comparatively analysed after the training phase with the EMG artificial amplification method described previously (Cheron et al., 1996): for each muscle input the rectified EMG signal was selectively amplified ($\times 2$) during two dedicated phases (the major stance phase (STP), between 35 and 52% of the gait cycle (200 ms), and the major swing phase (SWP), between 72 and 90% of the gait cycle (200 ms)).

Fig. 4 illustrates this method for the SOL muscle selectively amplified during the STP. The superimposition of the original (learned) EMG and the amplified one (Fig. 4A) is aligned to the corresponding velocity profile of the thigh, shank and foot (Fig. 4B–D, respectively). In order to quantify the effect of the artificial modification of the EMG on the velocity profile we systematically subtracted the initial curve to the modified one. Then for each of the ten different learnings the resulting curves were superimposed (Fig. 4E–G). This display documents the reproducibility of the identification process for the illustrated muscle (SOL). For the initial maximal peaks of these curves, peaks occurred in the same direction in 90, 50 and 100% of the curves for the thigh, shank and foot respectively. These percentages can be interpreted like a reproducibility score (RS). The same type of analysis was performed for all the muscles (Table 2) and for the EMG modifications performed during the stance and the swing phase. The lowest score obtained was 50% reflecting that half of the curves peak to one direction whereas the other half peak to the opposite direction.

In order to assess whether the experimental population exhibited significant reproducibility, we compared observed RSs with the ones produced by a fictive population composed of series of ten learning trials displaying a random identification process. For one particular series of ten random learning trials, the probability (P_{100}) of having ten times the same functional identification of the modification of one EMG is given by:

$$P_{100} = \frac{C_2^1}{2^{10}} = \frac{2}{1024} = 0.0019 \text{ with } C_m^n = \frac{m!}{n!(m-n)!}$$

The other four probabilities are given by:

$$P_{90} = \frac{2 \cdot C_2^2 \cdot \dfrac{10!}{9!}}{2^{10}} = \frac{20}{1024} = 0.019$$

$$P_{80} = \frac{2 \cdot C_2^2 \cdot \dfrac{10!}{8! \cdot 2!}}{2^{10}} = \frac{90}{1024} = 0.087$$

$$P_{70} = \frac{2 \cdot C_2^2 \cdot \dfrac{10!}{7! \cdot 3!}}{2^{10}} = \frac{240}{1024} = 0.234$$

Table 3
Proportion of reproducibility scores in each population

Reproducibility score	100%	90%	80%	70%	60%	50%
Proportion in fictive population ($n = 1024$)	0.0019	0.019	0.087	0.234	0.410	0.246
Proportion in experimental population ($n = 36$)	0.388	0.361	0.110	0.027	0.053	0.055

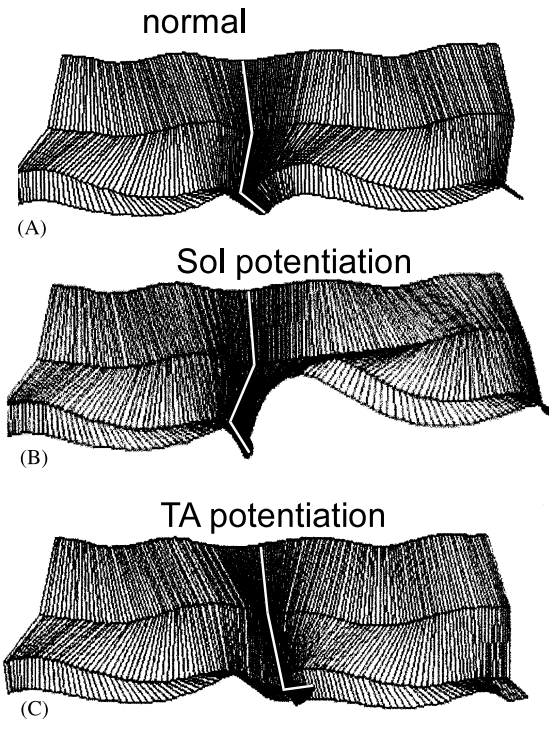

Fig. 5. (A–C) Sagittal stick diagrams of the lower limb kinematics obtained after DRNN learning of normal locomotion (A) and after artificial EMG potentiation of SOL (B) and TA (C) muscles.

$$P_{60} = \frac{C_2^2 \cdot \dfrac{10!}{6! \cdot 4!}}{2^{10}} = \frac{420}{1024} = 0.410$$

$$P_{50} = \frac{C_2^2 \cdot \dfrac{10!}{5! \cdot 5!}}{2^{10}} = \frac{252}{1024} = 0.246$$

Table 3 shows the proportions of the RSs encountered in the fictive and in the experimental populations. While 85.9% of the experimental RS values were higher or equal to 80%, only 10.7% of the fictive random RS values were higher or equal to 80%.

One-way analysis of variance (ANOVA) was used to compare the RSs obtained in the experimental population with those obtained in the fictive population. The RSs obtained for the SOL ($P < 0.0005$), TA ($P < 0.0005$), RF ($P < 0.001$) and VL ($P < 0.001$) muscles in the experimental population were significantly different from those obtained in the fictive population. Reproducibility of the identification process of the BF and the LG muscles was not better in the experimental than in the fictive population.

3.4. Biological plausibility

For each segment only two situations are possible: a forward or backward angle elevation. In order to test the physiological plausibility of the DRNN identification, the basic idea was to compare the angular directional change induced by artificial EMG potentiation of a single muscle with the physiological knowledge of the pulling direction of the muscle. This knowledge is easily accessible for mono-articular muscles, but is less straightforward for the pluri-articular muscles. In the latter, the muscle force can be involved in a force regulation process for which the directional action is not directly defined by the pulling direction of the muscle. Moreover, dynamical coupling between the three joint segments can be implicated in the evoked movement. For example, Fig. 5 illustrates the effect of SOL and TA artificial potentiation applied throughout the walking sequence on the sagittal lower limb kinogram over two steps. Whereas the former results in digitigrade gait (explained by the pulling action of SOL) with increased knee flexion (explained by a coupling action) more marked during the swing phase, the latter results in increased ankle dorsiflexion (walking on the heel explained by the pulling action of TA) and knee hyperextension (coupling action) more marked during the stance phase. The implications of such complex dynamical simulations of biomechanics and muscle coordination in human walking have been recently revisited by Zajac et al. (2003).

If we take into account the forward or backward direction of the movement induced by a specific EMG potentiation in comparison with the physiological action classically recognised for a specific muscle on a specific segment, we may introduce a physiological plausibility score (PPS). The idea is to calculate for the ten different learning sets the ratio between the sum of the physiological pulling actions produced by the EMG potentiation and the sum of the pulling and the non-pulling actions. This was quantified by means of the following equation:

$$\mathrm{PPS} = \frac{\sum V_{\mathrm{pull}}}{\left|\sum V_{\mathrm{pull}} + \sum V_{\mathrm{non\text{-}pull}}\right|}$$

where V_{pull} is the maximal amplitude of the first peak of the velocity profile directed to the physiological pulling action of the muscle. As used in the case of RS, this velocity profile results from the difference between the velocity profile induced by the EMG potentiation and the normal velocity profile. $V_{\mathrm{non\text{-}pull}}$ corresponds to the maximal amplitude of the first peak of the same type of velocity profile but directed to the non-pulling direction of the muscle. A PPS of 1.0 will mean that the EMG was interpreted by DRNN as producing the physiological pulling action of the muscle for the ten different learning. This was the case for the action of the SOL muscle on the foot segment during the SWP and for the VL action on the shank during the PPS (Table 4). The lowest scores (0.32 and 0.39) were obtained for the TA

Table 4
Physiological plausibility score (PPS) of the six analysed muscles (rectus femoris (RF), vastus lateralis (VL), biceps femoris (BF), gastrocnemius lateralis (GL), tibialis anterior (TA) and soleus (SOL)) with respect to their classically accepted pulling direction

Action on foot (PPS)			Action on shank (PPS)		
Muscle	STP	SWP	Muscle	STP	SWP
TA	0.94	0.32	VL	0.97	1.0
SOL	0.95	1.0	RF	0.75	0.69
GL	0.80	0.84	BF	0.39	0.82

during the SWP and the BF during the STP, respectively (Table 4).

4. Discussion

In the present study, it is demonstrated that the DRNN is able to reproduce a major parameter of lower limb kinematics in human locomotion (Lacquaniti et al., 1999; Cheron et al., 2001b) by using multiple raw EMG data. This dynamic mapping provides a new tool for understanding the functional relationships between multiple EMG profiles and the resulting movement. In the context of motor learning the DRNN may be considered as a model of biological learning mechanisms underlying motor adaptation (Cheron et al., 1996). According to Conditt et al. (1997), adaptation to change in human movement dynamics is achieved by neuronal modules. These modules realise learning through dynamic mapping between kinematic states (positions or velocities) and the forces associated with these states. The brain is thus capable of forming and memorising remarkably accurate internal representations of body segment dynamics (Conditt and Mussa-Ivaldi, 1999). This establishes a functional relation between force and motion, which is generally complex and non-linear (Zajac and Winters, 1990). Using artificial learning of the mapping between multiple EMG patterns and velocities of lower limb segments we found that the attractor states reached through learning correspond to biologically interpretable solutions. However, in its present form our method does not use force signals but only raw EMG signals. Force signals do not only depend on muscle activation signal reflected in the EMG but also on intrinsic properties of contractile apparatus and passive tissue contribution. Another problem results from dynamical laws of motion that produce kinematic output depending on muscle and external force and torque (see interaction torque, Gribble and Ostry, 1999; Bastian et al., 2000). These latter phenomena are not explicitly available as controlled variables but may interfere with the identification process of the DRNN. However, this neural network is able to decipher some motor strategies using interaction torque in multi-joint movements (unpublished data). For some authors, EMG patterns are a good reflection of the motor programme used by the CNS for controlling movement (Gottlieb, 1993). However, for others, EMG and kinematic patterns are emergent, non-programmable properties of the system and the control signals are positional in nature (Feldman et al., 1998; Gribble et al., 1998; McIntyre and Bizzi, 1993). In this controversial context the present method is not intended to propose a model for motor control based on feedforward related EMG signal for predicting kinematics. On the contrary, we propose to use the identification between EMG signals and kinematics for deciphering the complex relatonships between multiple muscular activation and the resulting movements, and also to expect to use this dynamic memory for prosthetic control.

A series of experimental locomotion studies have provided detailed evidence for the implication of elevation angles into coordinative laws leading to a reduction in kinematic degrees of freedom (Borghese et al., 1996; Bianchi et al., 1998a,b; Grasso et al., 1998, 1999, 2000; Cheron et al., 2001a,b; for a review, see Lacquaniti et al., 1999). The adaptive process of the DRNN may take advantage of this geometrical property in identifying the dynamics of a locomotor task in terms of the intrinsic coordinate system of the sensors and actuators.

The challenge of artificial neural network simulation of human locomotion is not only to reproduce the movement but also to reach biological interpretability. Our results show that the quality of the identification may allow to clearly interpret the role of each muscle in the stance and swing phases of locomotion. For this testing we applied a method developed previously (Cheron et al., 1996) for verifying the biological plausibility of the DRNN identification during complex figurative drawing without any previous indication about muscle action, anatomy or neural organisation. After the learning phase the same EMG inputs are fed to the DRNN with an amplitude magnification of a short sequence of one of these EMG inputs. This procedure discloses the direction of action of the muscle whose EMG is partly reinforced. As for drawing (Cheron et al., 1996), the DRNN was able to recognise the preferential action of most muscles in walking.

With this method of direct amplification of an arbitrary portion of EMG signals, variations related to the physiological complexity of the signal can be expected. This drawback can be partly overcome by selecting more EMG portions. The advantage of using complex EMG signals rather than pulse profile simplification is that it is closer to the original waveform of the neurophysiological signals in which both reflex and central command could be identified in selected situations (Horita et al., 2002).

Taking into account the fact that our model presents two types of adaptive parameters, namely the combinatory of synaptic weights and time constants of each neuronal unit, and the possibility for degrees of freedom in parametric determination of the supervisor learning process, we tested the reproducibility and quality of the identification process. For this, identical EMG inputs and kinematic outputs were used for performing ten successive learning identifications. For each one of these, only the initial weight random distribution was changed. This procedure demonstrated that although different identification states can be obtained with the same learning scores (asymptotical error reaching 0.001) (Fig. 4F), some invariant profiles can emerge from the mapping process (Fig. 4E and G). The procedure also allowed to eventually reject cases of non-physiological identification characterised by divergence. These occurrences can be partly explained by (1) the limited number of muscles used in the mapping (six muscles whereas more than 50 muscles are implicated in a single lower limb during locomotion (Yamaguchi et al., 1990)); (2) the absence in the present DRNN of explicit knowledge about anatomy and physiology of muscle acting as eccentric or concentric actuator for providing forces; (3) the absence of the passive contribution of non-muscular elements (e.g. preflex components (Dickinson et al., 2000)). The DRNN identification would probably be improved by increasing the number of recorded muscles including deeper muscles, and by introducing biological EMG filters and sign-adjusted EMG transformation depending of the eccentric or concentric action of the muscle as demonstrated for the upper limb movement (Draye et al., 1997). However, transformations of the raw EMG signals by kinematics-related data such as those based on Hill's model suffer from the fact that output elements contaminate the original neuronal input. This problem is particularly crucial if the DRNN is used to study the spontaneous emergence of multiple attractor states linked to the basic input–output mapping. For example, the distribution of the time constants associated with each neurone-like unit may differ in function of the type of movement, giving rise to tonic and phasic hidden neurones (Draye et al., 2002). Reciprocity and modularity may also arise naturally through correlations in the activation states of recurrent networks (Hua et al., 1999). As the EMG patterns comprise both feedback and feedforward guided sequences, after learning the DRNN output can provide control signals comparable to those produced by the central pattern generators for which hybrid feedforward/feedback systems have been proposed as optimal controller for rhythmic movements (Kuo, 2002). The present approach might therefore also be of benefit for the potential use of the DRNN in prosthetic control (Craelius, 2002). In particular, the DRNN could be used as a dynamically adaptive interface between actual EMG signals from residual muscles and artficial actuators command. The DRNN would be dedicated to a repertoire of learned movements with generalised properties in order to build a patient-specific dynamical memory of motor behaviour.

Acknowledgements

We thank Paul Demaret and Marie Dufief for technical assistance and Michelle Plasch for secretarial assistance. This work was supported by the Belgian National Fund for Scientific Research (F. N. R. S.), the Research Fund of the University of Brussels (U. L. B.), the General Directorate of Technology, Research and Energy of the Wallon government, the Artemi SA and Protechnik SA. F. Leurs is supported by the Ministry of Research of Luxembourg.

References

Bastian AJ, Zackowski KM, Thach WT. Cerebellar ataxia: torque deficiency or torque mismatch between joints? J Neurophysiol 2000;83:3019–30.

Bianchi L, Angelini D, Orani GP, Lacquaniti F. Kinematic coordination in human gait: relation to mechanical energy cost. J Neurophysiol 1998a;79:2155–70.

Bianchi L, Angelini D, Lacquaniti F. Individual characteristics of human walking mechanics. Pflugers Arch 1998b;436:343–56.

Borghese NA, Bianchi L, Lacquaniti F. Kinematic determinants of human locomotion. J Physiol 1996;494:863–79.

Cheron G, Draye JP, Bourgeois M, Libert G. A dynamic neural network identification of electromyography and arm trajectory relationship during complex movements. IEEE Trans Biomed Eng 1996;43:552–8.

Cheron G, Bengoetxea A, Bouillot E, Lacquaniti F, Dan B. Early emergence of temporal co-ordination of lower limb segments elevation angles in human locomotion. Neurosci Lett 2001a;308:123–7.

Cheron G, Bouillot E, Dan B, Bengoetxea A, Draye JP, Lacquaniti F. Development of a kinematic coordination pattern in toddler locomotion: planar covariation. Exp Brain Res 2001b;137:455–66.

Conditt MA, Mussa-Ivaldi FA. Central representation of time during motor learning. Proc Natl Acad Sci USA 1999;96:11625–30.

Conditt MA, Gandolfo F, Mussa-Ivaldi FA. The motor system does not learn the dynamics of the arm by rote memorization of past experience. J Neurophysiol 1997;78:554–60.

Craelius W. The bionic man: restoring mobility. Science 2002;295:1018–21.

Dickinson MH, Farley CT, Full RJ, Koehl MA, Kram R, Lehman S. How animals move: an integrative view. Science 2000;288:100–6.

Doya K. Universality of fully connected recurrent neural networks. Technical report. University of California: San Diego, 1993.

Draye JP, Pavisic D, Cheron G, Libert G. Adaptative time constant improved the prediction capacity of recurrent neural network. Neural Process Lett 1995;2:1–5.

Draye JP, Pavisic D, Cheron G, Libert G. Dynamic recurrent neural networks: a dynamical analysis. IEEE Trans Syst Man Cyber 1996;26:692–706.

Draye JP, Cheron G, Pavisic D, Libert G. Improved identification of the human shoulder kinematics with muscle biological filters. 1211.

In: Keravnou E, Garbay C, Baud R, Wyatt J, editors. Lecture Notes in Artificial Intelligence. Berlin: Springer, 2003:417–29.

Draye JP. Recurrent neural networks: properties and models. In: Masterbroek HAK, Vos JED, editors. Plausible Neural Networks for Biological Modelling. Dordrecht: Kluwer Academic Publishers, 2001:49–74.

Draye JP, Winters JM, Cheron G. Self-selected modular recurrent neural networks with postural and inertial subnetworks applied to complex movements. Biol Cybern 2002;87:27–39.

Feldman AG, Ostry DJ, Levin MF, Gribble PL, Mitnitski AB. Recent tests of the equilibrium-point hypothesis (lambda model). Motor Control 1998;2:189–205.

Gottlieb GL. A computational model of the simplest motor program. J Mot Behav 1993;25:153–61.

Ferrigno G, Pedotti A. ELITE: a digital dedicated hardware system for movement analysis via real-time TV signal processing. IEEE Trans Biomed Eng 1985;32:943–50.

Grasso R, Bianchi L, Lacquaniti F. Motor patterns for human gait: backward versus forward locomotion. J Neurophysiol 1998;80:1868–85.

Grasso R, Peppe A, Stratta F, Angelini D, Zago M, Stanzione P, Lacquaniti F. Basal ganglia and gait control: apomorphine administration and internal pallidum stimulation in Parkinson's disease. Exp Brain Res 1999;126:139–48.

Grasso R, Ivanenko YP, McIntyre J, Viaud-Delmon I, Berthoz A. Spatial, not temporal cues drive predictive orienting movements during navigation: a virtual reality study. Cogn Neurosci 2000;11:775–8.

Gribble PL, Ostry DJ. Compensation for interaction torques during single-and multijoint limb movement. J Neurophysiol 1999;82:2310–26.

Gribble PL, Ostry DJ, Sanguineti V, Laboissiere R. Are complex control signals required for human arm movement? J Neurophysiol 1998;79:1409–24.

Horita T, Komi PV, Nicol C, Kyrolainen H. Interaction between pre-landing activities and stiffness regulation of the knee joint musculoskeletal system in the drop jump: implications to performance. Eur J Appl Physiol 2002;88:76–84.

Hornik K, Stinchcombe M, White H. Multilayer feedforward networks are universal approximators. Neural Networks 1989;2:359–66.

Hua SE, Houk JC, Mussa-Ivaldi FA. Emergence of symmetric, modular, and reciprocal connections in recurrent networks with Hebbian learning. Biol Cybern 1999;81:211–25.

Kelso JA. Dynamic Patterns. The Self-Organization of Brain and Behavior. Cambridge: MIT Press, 1995:334.

Koike Y, Kawato M. Estimation of arm posture in 3D-Space from surface EMG signals using a neural network model. IEICE Trans Inf Syst 1994;E77-D:368–75.

Koike Y, Kawato M. Estimation of dynamic joint torques and trajectory formation from surface electromyography signals using a neural network model. Biol Cybern 1995;73:291–300.

Kuo AD. The relative roles of feedforward and feedback in the control of rhythmic movements. Motor Control 2002;6:129–45.

Lacquaniti F, Grasso R, Zago M. Motor patterns in walking. News Physiol Sci 1999;14:168–74.

McIntyre J, Bizzi E. Servo hypotheses for the biological control of movement. J Mot Behav 1993;25:193–202.

Neptune RR, Kautz SA, Zajac FE. Contributions of the individual ankle plantar flexors to support, forward progression and swing initiation during walking. J Biomech 2001;34:1387–98.

Pearlmutter BA. Learning state space trajectories in recurrent neural networks. Neural Comput 1989;1:263–9.

Savelberg HCM, Herzog W. Prediction of dynamic tendon forces from electromyographic signals: an artificial neural network approach. J Neurosci Methods 1997;78:65–74.

Sepulveda F, Wells DM, Vaughan CL. A neural network representation of electromyography and joint dynamics in human gait. J Biomech 1993;26:101–9.

Scholz JP, Kelso JAS. Intentional switching between patterns of bimanual coordination is dependent on the intrinsic dynamics of the patterns. J Motor Behav 1990;22:198–224.

Silva FM, Almeida LB. Speeding up backpropagation. In: Eckmiller R, editor. Advanced Neural Computers. Amsterdam: Elsevier, 1990:151–8.

Soechting JF, Flanders M. Evaluating an integrated musculoskeletal model of the human arm. J Biomech Eng 1997;119:93–102.

Yamaguchi GT, Sawa AGU, Moran DW, Fessler JM, Winters JM. A survey of human musculotendon actuator parameters. In: Winters JM, Woo SLY, editors. Multiple Muscle Systems: Biomechanics and Movement Organization. New York: Springer-Verlag, 1990:717–73.

Zajac FE, Winters JM. Modeling musculoskeletal movement systems: joint and body segmental dynamics, musculoskeletal actuation, and neuromuscular control. In: Winters JM, Woo SLY, editors. Multiple Muscle Systems: Biomechanics and Movement Organization. New York: Springer-Verlag, 1990:121–48.

Zajac FE, Neptune RR, Kautz SA. Biomechanics and muscle coordination of human walking. Part II: Lessons from dynamical simulations and clinical implications. Gait Posture 2003;17:1–17.